Spectrochimica Acta Part A: Molecular and Biomolecular Spectroscopy 248 (2021) 119196

Contents lists available at ScienceDirect

Spectrochimica Acta Part A: Molecular and Biomolecular Spectroscopy

journal homepage: www.elsevier.com/locate/saa

Bjurböle L/LL4 ordinary chondrite properties studied by Raman spectroscopy, X-ray diffraction, magnetization measurements and Mössbauer spectroscopy

A.A. Maksimova [a,b], E.V. Petrova [a], A.V. Chukin [a], B.A. Nogueira [c], R. Fausto [c], Á. Szabó [d,e], Z. Dankházi [e], I. Felner [f], M. Gritsevich [g,h], T. Kohout [i], E. Kuzmann [j], Z. Homonnay [j], M.I. Oshtrakh [a,*]

[a] Institute of Physics and Technology, Ural Federal University, Ekaterinburg 620002, Russian Federation
[b] The Zavaritsky Institute of Geology and Geochemistry of the Ural Branch of the Russian Academy of Sciences, Ekaterinburg 620016, Russian Federation
[c] CQC, Department of Chemistry, University of Coimbra, 3004-535 Coimbra, Portugal
[d] Lithosphere Fluid Research Laboratory, Eötvös Loránd University, Budapest, Hungary
[e] Department of Materials Physics, Eötvös Loránd University, Budapest, Hungary
[f] Racah Institute of Physics, The Hebrew University, Jerusalem 91904 Israel
[g] Finnish Geospatial Research Institute, Geodeetinrinne 2, 02430 Masala, Finland
[h] Department of Physics, University of Helsinki, Gustaf Hällströmin katu 2, P.O. Box 64, FI-00014 Helsinki, Finland
[i] Department of Geosciences and Geography, University of Helsinki, Gustaf Hällströmin katu 2, P.O. Box 64, FI-00014 Helsinki, Finland
[j] Laboratory of Nuclear Chemistry, Institute of Chemistry, Eötvös Loránd University, Budapest, Hungary

HIGHLIGHTS

- Raman spectroscopy detected higher contents of forsterite and enstatite in Bjurböle.
- The saturation magnetic moment for Bjurböle is ~7 emu/g.
- Fe^{2+} occupancies of M1 and M2 sites are determined by XRD and Mössbauer spectroscopy.

GRAPHICAL ABSTRACT

Bjurböle L/LL4 ordinary chondrite: the Raman spectra of olivine (***a***) and orthopyroxene (***b***), the Mössbauer spectrum of the bulk material (***c***) and classification of meteorite using Mössbauer parameters (***d***).

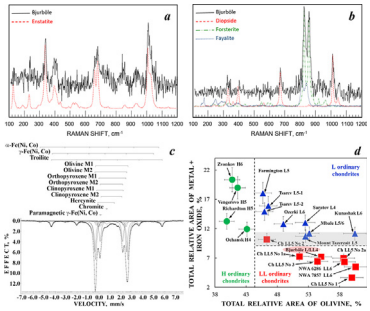

ARTICLE INFO

Article history:
Received 13 August 2020
Received in revised form 26 October 2020
Accepted 4 November 2020
Available online 13 November 2020

Keywords:
Bjurböle L/LL4 ordinary chondrite
Raman spectroscopy
X-ray diffraction

ABSTRACT

Bjurböle L/LL4 ordinary chondrite was studied using scanning electron microscopy with energy dispersive spectroscopy, Raman spectroscopy, X-ray diffraction, magnetization measurements and Mössbauer spectroscopy. The phase composition and the relative iron fractions in the iron-bearing phases were determined. The unit cell parameters for olivine, orthopyroxene and clinopyroxene are similar to those observed in the other ordinary chondrites. The higher contents of forsterite and enstatite were detected by Raman spectroscopy. Magnetization measurements showed that the temperature of the ferrimagnetic-paramagnetic phase transition in chromite is around 57 K and the saturation magnetic moment is ~7 emu/g. The values of the ^{57}Fe hyperfine parameters for all components in the Bjurböle Mössbauer spectrum were determined and related to the corresponding iron-bearing phases. The relative iron fractions in Bjurböle and the ^{57}Fe hyperfine parameters of olivine, orthopyroxene and troilite were

* Corresponding author.
E-mail address: oshtrakh@gmail.com (M.I. Oshtrakh).

https://doi.org/10.1016/j.saa.2020.119196

Magnetization measurements
Mössbauer spectroscopy

compared with the data obtained for the selected L and LL ordinary chondrites. The Fe^{2+} occupancies of the M1 and M2 sites in silicate crystals were determined using both X-ray diffraction and Mössbauer spectroscopy. Then, the temperatures of equilibrium cation distribution were determined, using two independent techniques, for olivine as 666 K and 850 K, respectively, and for orthopyroxene as 958 K and 1136 K, respectively. Implications of X-ray diffraction, magnetization measurements and Mössbauer spectroscopy data for the classification of the studied Bjurböle material indicate its composition being close to the LL group of ordinary chondrites.

1. Introduction

Meteorites represent a unique opportunity to sample remnants of accretionary products of the early Solar System. They are classified according to their mineralogical, petrological, chemical, and isotopic properties and are divided into three main groups: iron, stony-iron, and stony meteorites. The stony meteorites are further classified as chondrites (that have not experienced igneous processing) or achondrites (that have a complex origin involving asteroidal or planetary differentiation). Stony meteorites are a subject of intense scientific investigations. Their diversity provides unprecedented possibilities for insights into the earliest history and evolution of the Solar System.

The Bjurböle meteorite fall occurred late in the evening on 12 March 1899 near Bjurböle, 6 km south from Porvoo, Finland, with the estimated impact site coordinates of 60° 20.42′ N and 25° 42.30′ E [1]. Bjurböle is the largest known meteorite recovered in Finland so far. A single mass fell into the ~1 m thick sea ice, making ~4 m wide hole in the ice and breaking into fragments due to the ground impact [1,2]. In total, over 328 kg of Bjurböle meteorite fragments were recovered. The main mass (over 80 kg) is currently on display at the Finnish Museum of Natural History at the University of Helsinki. The recovered fragments are unusually friable. Bjurböle is classified as an L/LL4 ordinary chondrite of shock level S1 and weathering index W0. This information can be found in the Meteoritical Bulletin Database and in two Internet sites (see [3–5]) but it has never been published in *Meteoritical Bulletin*.

Bjurböle is the most massive among the only 21 ordinary chondrites classified as L/LL4, being also the most recent and so far within only 3 L/LL4 cases which were witnessed as a meteorite fall. This subgroup of ordinary chondrites is of interest as one of the primitive bodies which contain chondrules, the crystallization products of silicate melt droplets, whose formation and metamorphism provide clues about the earlier history of the Solar System. Therefore, earlier studies of the Bjurböle L/LL4 meteorite were mostly related to chondrules, trace elements and isotope composition analyses (see, e.g., [6–11]). Studies of the chemical composition of the Bjurböle L/LL4 meteorite showed that olivine (Fe, $Mg)_2SiO_4$, as a solid solution of fayalite Fe_2SiO_4 (Fa) and forsterite Mg_2SiO_4, contains Fa of 26 mol% [12] and 26.2 mol% [13]. Later, a composition of orthopyroxene (Fe, Mg)SiO_3, as a solid solution of ferrosilite $FeSiO_3$ (Fs) and enstatite $MgSiO_3$, was studied. The Fs and Fa values were determined as 20.7 mol% and 26.2 mol%, respectively [14]. Additionally, magnetic measurements were done for the Bjurböle meteorite (see, e.g., [15–18] and references therein). The deduced saturation magnetic moment M_S of the Bjurböle L/LL4 was 20.55 emu/g [18].

Mössbauer spectroscopy was also applied to study the Bjurböle L/LL4 meteorite. The first study was dedicated to analyzing the iron content in the crystallographically nonequivalent M1 and M2 sites in extracted orthopyroxene and showed that the peak intensities ratio for the M1 and M2 sites is 0.46 [19]. Later, Mössbauer spectroscopy was used for ordinary chondrites classification (including Bjurböle L/LL4) but no Mössbauer parameters were presented [20]. Recent Mössbauer investigation of the several LL ordinary chondrites, including Bjurböle L/LL4, was directed to the study of troilite FeS, the spectral component of which was fitted using the full static Hamiltonian [21]. The authors determined for the troilite component in Bjurböle that: (i) the relative area *A* is 10.6% and (ii) the magnetic hyperfine field H_{eff} is 300 kOe. In addition, they also revealed the presence of chromite $FeCr_2O_4$, pyrrhotite (nonstoichiometric troilite $Fe_{1-x}S$), kamacite (α-Fe(Ni, Co) phase), olivine, orthopyroxene and ferric compound. However, they did not reveal the spectral components related to the ^{57}Fe in the M1 and M2 sites in silicate crystals [21]. In contrast, the possibilities of Mössbauer spectroscopy to identify spectral components associated with the M1 and M2 sites in olivine, orthopyroxene and clinopyroxene as well as with the minor components such as chromite, hercynite $FeAl_2O_4$, ferromagnetic α-Fe(Ni, Co), α_2-Fe(Ni, Co) and γ-Fe(Ni, Co) and paramagnetic γ-Fe(Ni, Co) phases and some other compounds have already been demonstrated [22–27]. Therefore, in this work we present the new results of our comprehensive study of the Bjurböle L/LL4 meteorite using scanning electron microscopy (SEM) with energy dispersive spectroscopy (EDS), Raman spectroscopy, X-ray diffraction (XRD), magnetization measurements and Mössbauer spectroscopy.

2. Materials and methods

Several small pieces of the Bjurböle L/LL4 ordinary chondrite were provided by the University of Helsinki (Helsinki, Finland) for the sample preparation at the Ural Federal University (Ekaterinburg, Russian Federation) and various investigations. Pieces of Bjurböle L/LL4 are very friable (Fig. 1a) and cannot be used to prepare a polished section. Therefore, part of the material was crushed and glued by epoxy and then polished by the standard method for SEM with EDS analysis and Raman spectroscopy (Fig. 1b). The other piece of Bjurböle L/LL4 was powdered for XRD, magnetization measurements and Mössbauer spectroscopy. About 200 mg was used for XRD measurement while only few mg was needed for magnetization measurements. For Mössbauer spectroscopy, ~120 mg of the powder was glued on thin Al foil (free from Fe) with a diameter of 2 cm. Considering the total Fe content of 20.6% [14], the sample thickness is of ~8 mg Fe/cm^2.

SEM characterization of the Bjurböle L/LL4 polished section was done in the two laboratories: (i) at the Ural Federal University by a ΣIGMA VP scanning electron microscope (Carl Zeiss), using an accelerating potential of 20 kV and a probe current of 461 pA, with an X-max (Oxford Instruments) EDS device and (ii) at the Eötvös Loránd University by a FEI Quanta 3D scanning electron microscope, using an accelerating potential of 20 kV and a probe current of 16 nA, with EDAX Apollo XP SDD EDS detector (acquisition time of the EDS measurements was set to 20 s).

The Raman spectra were measured with an acquisition time of 10 s and 10 accumulations using a Horiba LabRam HR Evolution micro-Raman system at the University of Coimbra with a 50× magnification objective (NA = 0.75). Laser excitation was

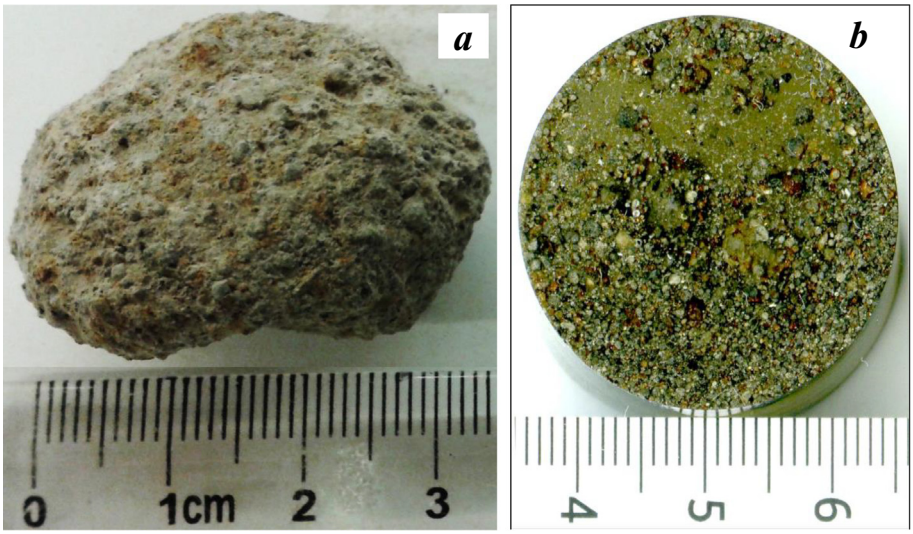

Fig. 1. A piece of the Bjurböle L/LL4 ordinary chondrite (***a***) and polished section prepared from the crashed Bjurböle L/LL4 matter glued with epoxy (***b***).

performed at 532 nm (~2 mW at the sample). The used spectral resolution was 1.5 cm^{-1} and the spot size was ~1 μm.

Powder XRD analysis of Bjurböle L/LL4 was done at the Ural Federal University using an XRD–7000 powder diffractometer (Shimadzu) operating at 40 kV and 30 mA with CuK_α radiation using a graphite monochromator. Scanning was performed over 2Θ from 14° to 100°, with a step of 0.03° per 10 s. XRD pattern was processed using the Panalytical X'Pert High Score Plus (version 2.2c) software. The X-ray data were fitted by the least squares procedure using the Rietveld full profile refinements program. This Rietveld implementation is based on the source code of the modified version of the LHPM program [28]. The least squares refinements were performed with pseudo Voigt peak profiles. The phase composition was evaluated using the ICDD PDF-2 database. Then, initial structural parameters, atomic positions and temperature factors for the refinements were taken from the ICSD database. The quality of the refinement was evaluated by indices characterizing the fitting model: R_P = 2.52; R_{WP} = 3.44; R_{EXP} = 1.85; GOF (goodness of fit) = 3.46, whose values demonstrate its good quality, which allows an estimation of phase compositions up to the first decimal digit.

Magnetization measurements of Bjurböle L/LL4 were performed at the Hebrew University, using a commercial SQUID magnetometer MPMS-5S (Quantum Design) in the temperature range between 5 and 300 K. The differential SQUID sensitivity was 10^{-7} emu. The magnetometer was adjusted to be in a real zero magnetic field (H = 0) state prior to recording the zero-field-cooled (ZFC) curve. The sample was first cooled to 5 K at H = 0 Oe, then, the magnetic field H = 50 Oe was switched on to trace the ZFC branch of the magnetization $M(T)$ curves. Next, the field-cooled (FC) $M(T)$ branch was measured *via* heating from 5 to 300 K. The isothermal magnetization $M(H)$ curves were measured at 5, 150 and 295 K with applied magnetic fields up to 32 kOe.

The ^{57}Fe Mössbauer spectrum of Bjurböle L/LL4 was measured at the Ural Federal University using an automated precision developed in-house Mössbauer spectrometric system based on the SM-2201 spectrometer. This spectrometer operates with a saw-tooth shape velocity reference signal with quantification in 4096 steps. This velocity signal is formed by a digital-analog converter using discretization of 2^{12}. This spectrometer (due to the increase in the number of experimental spectrum points) provides much better adjustment to resonance and significantly increases the spectra quality as well as the analytical possibilities of Mössbauer spectroscopy to reveal major and minor spectral components in the complex spectra. However, this significantly increases the measurement time. The details and characteristics of this spectrometer and the system as well as its advances were described elsewhere (see [29,30] and references therein). The 1.8 × 10^9 Bq ^{57}Co(Rh) source (Ritverc GmbH, St. Petersburg) was at room temperature. The Mössbauer spectrum of Bjurböle L/LL4 was measured in transmission geometry with moving absorber at 295 K and recorded in 4096 channels. Then, this spectrum was converted into 1024-channel spectrum, by a consequent summation of four neighboring channels, to increase the signal-to-noise ratio for the minor spectral components. Statistics in the obtained spectrum was ~10.5 × 10^6 counts per channels and the signal-to-noise ratio was 436. The Mössbauer spectrum was measured over a period of 11 days, in order to reach the appropriate signal-to-noise ratio and obtain a reliable fit.

The Mössbauer spectrum of Bjurböle L/LL4 was fitted using UNIVEM-MS program with the least square procedure using a Lorentzian line shape. The line shape of the 1024-channel Mössbauer spectrum of the reference absorber of α-Fe foil with a thickness of 7 μm was pure Lorentzian with line widths (Γ, the full width at a half maximum) of $\Gamma_{1,6}$ = 0.218 ± 0.029 mm/s, $\Gamma_{2,5}$ = 0.216 ± 0.02 9 mm/s and $\Gamma_{3,4}$ = 0.209 ± 0.029 mm/s for the 1st and the 6th, the 2nd and the 5th, and the 3rd and the 4th peaks in the measured sextet, respectively. The velocity resolution (velocity per one channel) in the 1024-channel Mössbauer spectrum was ~0.014 mm/s per channel. Mössbauer parameters such as isomer shift, δ, quadrupole splitting, ΔE_Q, quadrupole shift for magnetically split components, ε ($2\varepsilon = \Delta E_Q$), magnetic hyperfine field, H_{eff}, line width, Γ, relative subspectrum (component) area, A, and normalized statistical quality of the fit, χ^2, were determined.

The Mössbauer spectrum of Bjurböle L/LL4 was fitted using the recently developed model which accounting for the spectral components related to the ^{57}Fe in the crystallographically non-equivalent M1 and M2 sites in olivine, orthopyroxene and clinopyroxene, and components related to α- and γ-phases in metallic Fe-Ni-Co alloy with variations in Ni concentration, chromite and hercynite. Moreover, a simulation of the full static Hamiltonian was applied for the troilite spectral component fit. The latter results in deducing more reliable Mössbauer parameters for the minor spectral components and overcomes the problem with fitting the troilite FeS component using the full static Hamiltonian in the complex Mössbauer spectra of ordinary chondrites (see [24,31]

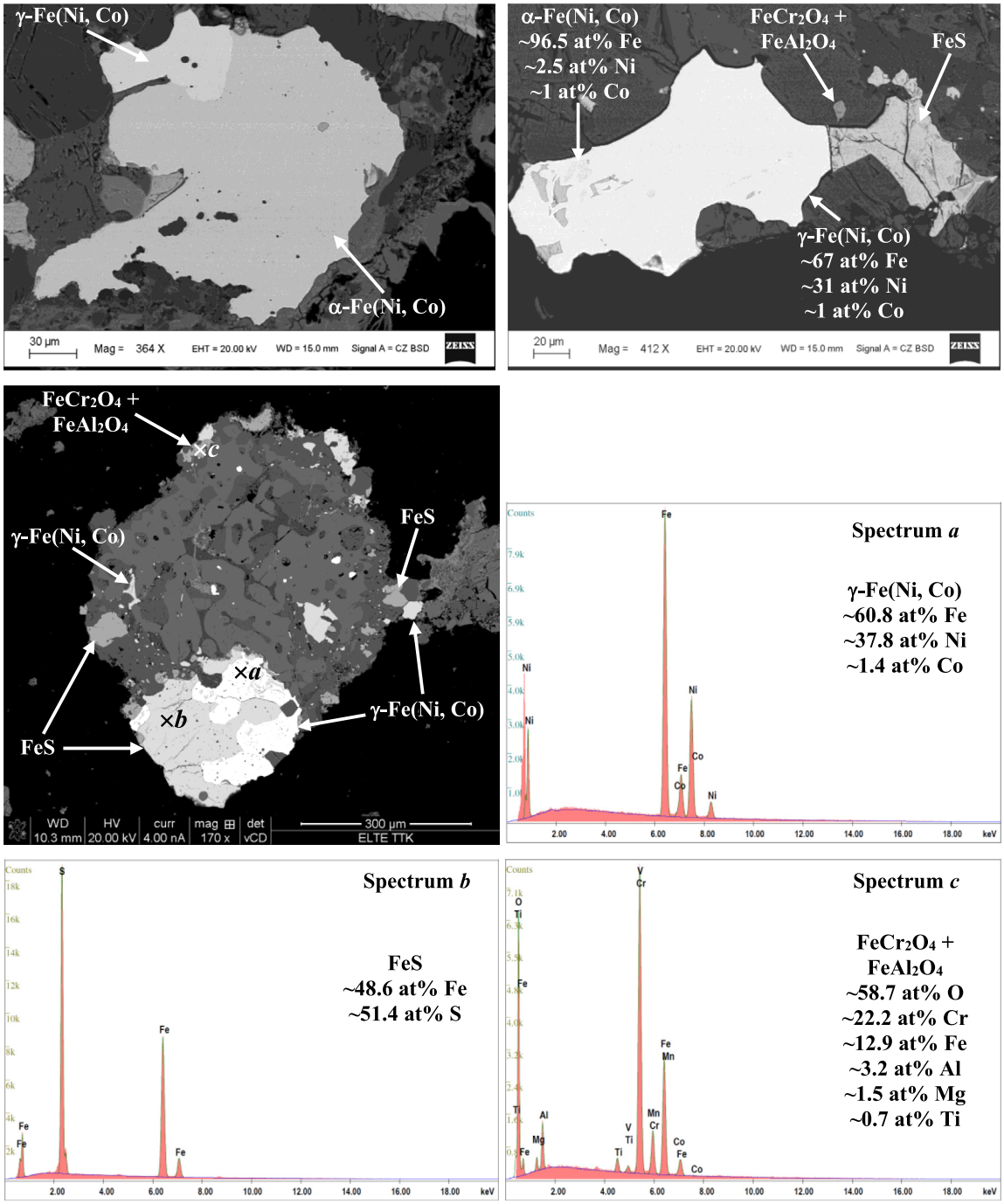

Fig. 2. Selected scanning electron microscopy images and energy dispersive spectra of the Bjurböle L/LL4 polished section. Symbol "×" and letters "***a***", "***b***" and "***c***" indicate the point of corresponding energy dispersive spectrum. The phases and their concentrations were determined by EDS.

and references therein). This fitting model was reported in [32] and applied for various ordinary chondrite spectra (see, e.g., [33–36]). Criteria of the best fit were the differential spectrum (the difference between experimental and calculated spectral points), χ^2 and the physical meaning of the parameters.

The instrumental (systematic) error for each spectral point was equivalent to ± 0.5 channel (in the velocity scale) and that to ±1 channel for the hyperfine parameters (in mm/s or kOe). If an error calculated with the fitting procedure (fitting error) for these parameters exceeded the instrumental (systematic) error, the larger error was used instead. The values of *A* are given as calculated in the fit with two decimal digits to keep the total relative area equal to 100%. The estimated relative error for *A* usually did not exceed 10%. Values of δ are given relative to α-Fe at 295 K.

3. Results and discussion

3.1. Characterization by scanning electron microscopy

The selected SEM images and EDS chemical analysis of the Bjurböle L/LL4 polished section are shown in Fig. 2. Ranges and averaged values of metals, sulfur and oxygen concentrations in the minor iron-bearing phases are given in Table 1. SEM images show the metal grains which consist of α-Fe(Ni, Co) or γ-Fe(Ni, Co)

Table 1
Ranges and averaged concentrations of metals, sulfur and oxygen in selected minor iron-bearing phases in Bjurböle L/LL4 ordinary chondrite obtained using EDS.

Phase	Concentration, at%		
	Min	Max	Average
α-Fe(Ni, Co)			
Fe	91.6	96.3	93.9
Ni	2.1	6.5	4.1
Co	1.4	3.7	2.0
γ-Fe(Ni, Co)			
Fe	46.2	65.1	57.8
Ni	34.0	53.1	41.3
Co	0.5	1.3	0.9
γ-Fe(Ni, Co) par[a]			
Fe	65.0	68.6	66.3
Ni	30.2	33.9	32.7
Co	0.8	1.2	1.0
FeS			
Fe	47.2	51.5	50.1
S	48.5	52.8	50.0
$FeCr_2O_4$			
O	43.9	63.9	54.3
Cr	19.5	30.1	24.7
Fe	11.3	17.7	14.3
Al	2.7	4.2	3.5
Mg	1.3	2.4	1.8
Ti	0.5	1.1	0.8
$FeTiO_3$			
O	55.5	62.3	58.2
Ti	18.0	22.6	20.9
Fe	16.7	18.9	18.0
Mg	2.3	2.4	2.4

[a] **par** is the paramagnetic γ-Fe(Ni, Co) phase.

phases only as well as of both phases within one grain. The concentration ranges (Table 1) for the metal grains indicate the presence of the paramagnetic γ-Fe(Ni, Co) phase in addition to the ferromagnetic α-Fe(Ni, Co) and γ-Fe(Ni, Co) phases, but there were no grains with the ferromagnetic α_2-Fe(Ni, Co) phase. The metal grains are found in associations with troilite and chromite inclusions. Chromite inclusions contain about 3.5 at% of Al. That indicates the possible presence of hercynite in chromite grains caused by Cr substitution by Al. Two ilmenite inclusions are also observed in the section. Some metal grains demonstrate a complex mixture of different phases (α-Fe(Ni, Co), γ-Fe(Ni, Co) and γ-FeNi(Co) phases) with the concentration variations even within one phase as shown in Fig. 3. Similar metal grains were observed in the Northwest Africa (NWA) 6286 LL6 and NWA 7857 LL6 [34], Ozerki L6 [36] and Kemer L4 [37] ordinary chondrites. A formation of these metal grains in ordinary chondrites may occur according to the model described in [38].

3.2. Raman spectroscopy

In the Raman experiments, a series of points located in different regions of the meteorite sample was randomly defined and spectroscopically evaluated. Three different types of minerals were identified, which belong to the orthopyroxene, clinopyroxene and olivine families. Representative Raman spectra of Bjurböle L/LL4 are shown in Fig. 4, together with reference spectra [39] of the identified minerals. Fig. 4a shows the spectrum of the identified orthopyroxene in comparison with that of 100% enstatite. In the spectrum of Bjurböle L/LL4, the frequencies of the bands due to the Si–O stretching (1012 and 1032 cm^{-1}), Si–O bending (662 and 682 cm^{-1}) and (Mg, Fe)–O stretching (341 cm^{-1}) modes correspond to those of an orthopyroxene with a high content of enstatite [40]. In turn, the Raman spectrum of Bjurböle L/LL4 in Fig. 4b demonstrates the presence of olivine and clinopyroxene (diopside, $MgCaSi_2O_6$) in the meteorite. The major bands at 823 and 855 cm^{-1}, assigned to olivine, are ascribable to the Si–O symmetric and anti-symmetric stretching vibrations of this mineral, while minor bands at 919 and 961 cm^{-1} are also noticeable. All these bands appear at characteristic frequencies of olivine with a high content of forsterite [41,42]. On the other hand, the bands observed at 323, 393, 668, 1012 and 1051 cm^{-1} are assigned to diopside: the first two bands to SiO_4 tetrahedral tilting vibrations, the third to the Si–O–Si symmetric stretching mode involving the bridging oxygen atoms between the SiO_4 tetrahedral chains, and the last two bands to the O–Si–O symmetric and anti-symmetric vibrations within the SiO_4 tetrahedrals [43].

3.3. X-ray diffraction

XRD pattern of the Bjurböle L/LL4 meteorite is shown in Fig. 5. The phase composition of this material was determined by the Rietveld full profile analysis with ICDD cards (the results and corresponding ICDD card numbers are shown in Table 2). This phase composition is similar to that obtained for other ordinary chondrites, but the olivine and troilite contents were smaller, whereas the orthopyroxene and Ca-rich clinopyroxene contents were larger than those in the earlier studied NWA 6286 LL6 and NWA 7857 LL6 [34] and Ozerki L6 [36] meteorites. The observed Ca-rich clinopyroxene has the diopside structure which is in agreement with the Raman spectrum in Fig. 4b. The presence of hercynite in Bjurböle L/LL4 is shown by the XRD that confirms the results of chromite chemical analysis obtained by EDS, indicating the presence of Al in chromite inclusions (see Table 1) which can substitute Cr. The unit cell parameters for olivine, orthopyroxene and Ca-rich clinopyroxene are summarized in Table 3. These unit cell parameters are comparable with those obtained for the mentioned LL and L ordinary chondrites in [34,36].

3.4. Magnetization measurements

The temperature dependence of both ZFC and FC magnetization $M(T)$ curves measured at 50 Oe and the isothermal field dependence of the magnetization $M(H)$ measured at 5, 150 and 295 K for Bjurböle L/LL4 are displayed in Fig. 6. Both ZFC and FC plots indicate a multi-phase magnetic material. A pronounced peak at 57(1) K is obtained in ZFC plot and small steps in both branches are observed around 207(2) K (see insets in Fig. 6a). The sharp increase of both branches at low temperature (down to 5 K) indicates clearly the presence of a paramagnetic (PM) component. The peak at 57(1) K is related to the ferrimagnetic-paramagnetic phase transition of chromite [44] and fits well with the peaks at 59 and 58 K, obtained for NWA 6286 LL6 and NWA 7857 LL6 ordinary chondrites, respectively [34]. This fact may indicate similar compositions of chromite in these three meteorites. That is also in agreement with the EDS results shown here in Table 1 and in Table 1 in [34]. The step origin around 207(2) K is not known yet, but it also appears in the ZFC branch of the fusion crust of Kemer L4 [37].

The isothermal $M(H)$ curves confirm this picture. At 5 K, the magnetization first increases linearly up to 5000 Oe and then tends to saturate. This plot clearly reveals the admixture of magnetic and PM components and can be fitted as: $M(H) = M_S + \chi_p H$, where the saturation moment (corrected) M_S = 7.0(1) emu/g, is the intrinsic magnetic phases contribution, and $\chi_p H$ ($\chi_p = 6.9 \times 10^{-6}$ emu/g Oe) is the linear PM contribution (Fig. 6c). At 150 and 295 K (Fig. 6b), the PM contribution is low, and saturation is achieved at low applied fields. M_S at both temperatures is practically the same as at 5 K, indicating that the magnetic transition of the dominant phase(s) is well above room temperature. Moreover, the coercive fields H_C do not change much from 5 K (Fig. 6d) to

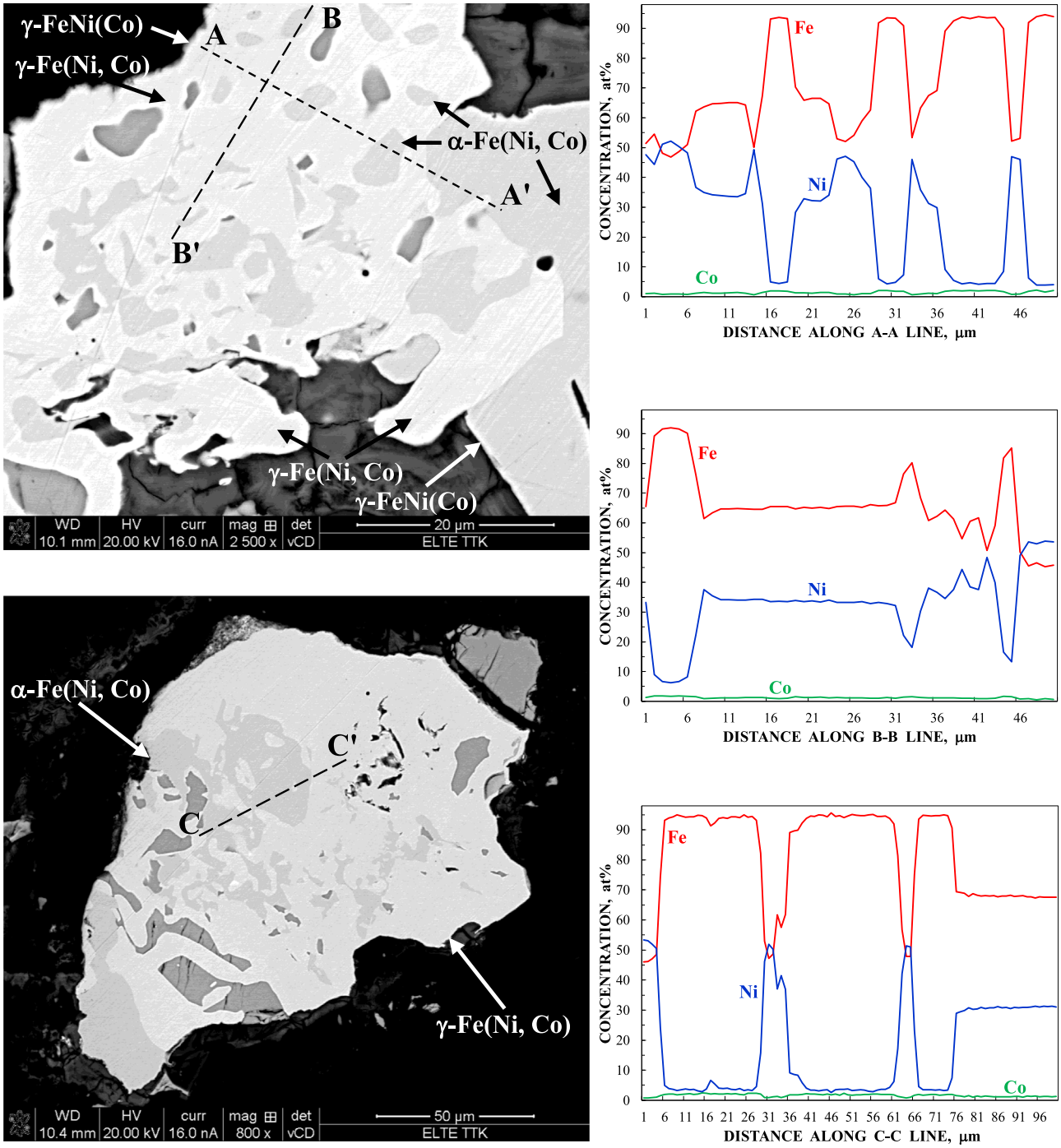

Fig. 3. Scanning electron microscopy images of selected metal grains with a complex phase composition and concentration variations of Fe, Ni and Co along the lines A–A′, B–B′ and C–C′ in these grains obtained using energy dispersive spectroscopy.

295 K (H_C = −200(10) Oe and H_C = −165(10) Oe, respectively), confirming this explanation. It should be noticed that the constant M_S value of ~7.0 emu/g deduced here in the temperature range 5–295 K is substantially smaller than M_S = 20.55 emu/g determined for Bjurböle L/LL4 in [18] but agrees well with the M_S values (at 5 K) of 5.42 and 8.8 emu/g observed for NWA 6286 LL6 and NWA 7857 LL6 ordinary chondrites, respectively [34].

3.5. Mössbauer spectroscopy

The Mössbauer spectrum of Bjurböle L/LL4 matter is shown in Fig. 7. This spectrum was fitted well using a superposition of: (i) three magnetic sextets, (ii) seven quadrupole doublets and (iii) two paramagnetic singlets. All Mössbauer parameters deduced are collected in Table 4. Optimal fit of the Mössbauer spectrum using this model is confirmed by the absence of any significant misfits at the differential spectrum and the lowest value of χ^2 = 1.355 in comparison with differential spectra and χ^2 values obtained for other fitting models. Using these ^{57}Fe hyperfine parameters, all components exhibited in Fig. 7 were assigned to the corresponding iron-bearing phases, in accordance with our previous studies [22–27,33–37].

The three pairs of quadrupole doublets with the largest ΔE_Q values were related to the M1 and M2 sites in olivine, orthopyroxene

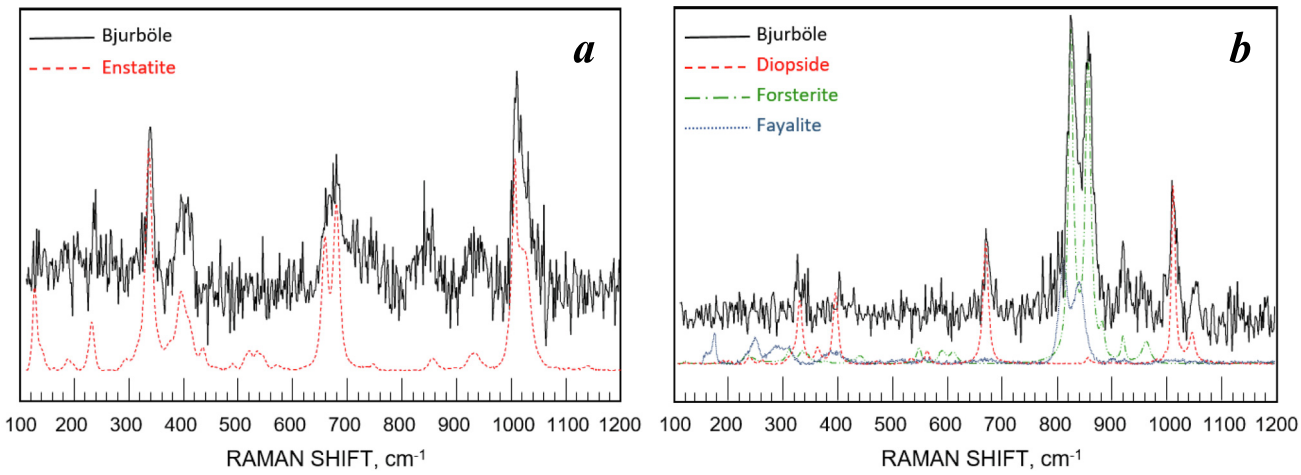

Fig. 4. Representative Raman spectra of the Bjurböle L/LL4 ordinary chondrite and reference spectra from [38] of the identified minerals.

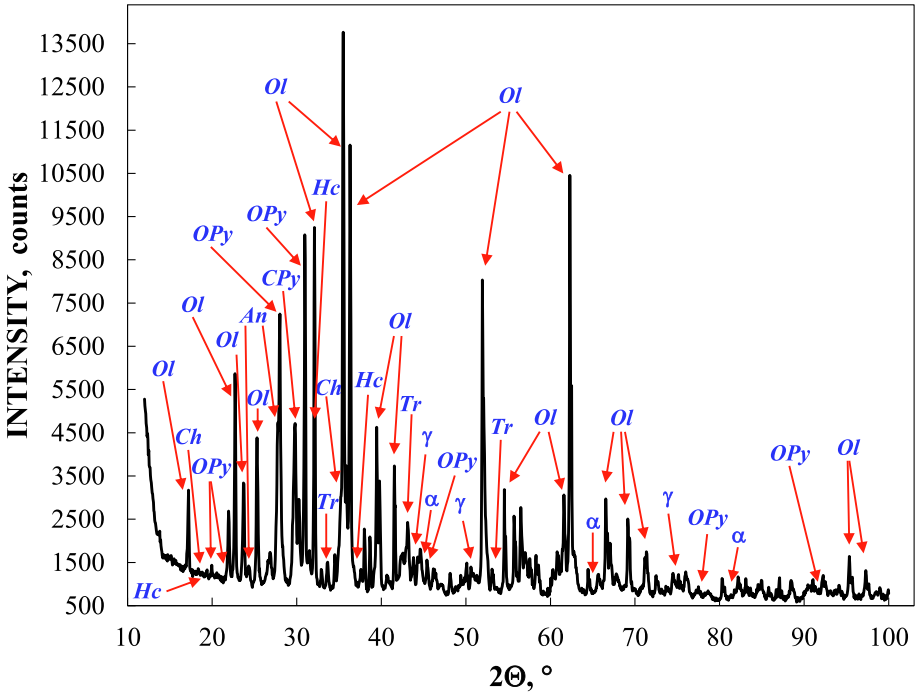

Fig. 5. X-ray diffraction pattern of the Bjurböle L/LL4 ordinary chondrite with selected phases: olivine (***Ol***), orthopyroxene (***OPy***), anorthite (***An***), Ca-rich clinopyroxene (***CPy***), troilite (***Tr***), γ-Fe(Ni, Co) phase (**γ**), α-Fe(Ni, Co) phase (**α**), chromite (***Ch***) and hercynite (***Hc***).

Table 2
Phase composition of the Bjurböle L/LL4 ordinary chondrite obtained by X-ray diffraction.

Phase	Content, wt%	ICDD card for reference
Olivine	47.5	01-080-1630
Orthopyroxene	26.2	01-083-0666
Anorthite	13.9	01-079-1149
Ca-rich clinopyroxene	6.9	01-083-0088
Troilite	2.4	01-080-1030
Chromite	1.8	00-034-0140
γ-Fe(Ni, Co)	0.7	01-089-4185
α-Fe(Ni, Co)	0.5	00-037-0474
Hercynite	0.1	00-034-0192

and clinopyroxene, respectively. The two magnetic sextets with the largest H_{eff} values were assigned to the α-Fe(Ni, Co) and γ-Fe (Ni, Co) phases, respectively. The total relative area of these sextets is ~4.5% only. That corresponds to LL ordinary chondrites and agrees with a small M_S value. However, the small content of ferromagnetic phases did not permit us to reveal more magnetic sextets, which may stem from Ni content variations within each phase, as shown by EDS (see Fig. 3). Therefore, the values of Γ for these sextets are slightly broad due to averaging of slightly different ^{57}Fe microenvironments in the α- and γ-phases. The small value of H_{eff} (~287 kOe) corresponds to the γ-FeNi and/or ordered γ-Fe(Ni, Co) phases (see [45]). That also agrees well with the presence of these phases in the metal grains shown by EDS (Table 1 and Fig. 3). The larger total relative area of the γ-phase than that for the α-phase correlates with the XRD data (see Table 2) and agrees well with earlier conclusion about a higher content of the γ-phase, which is enriched with Ni, in Bjurböle in comparison with other similar meteorites [14]. The δ value for the paramagnetic γ-Fe(Ni, Co) phase is similar to some δ values for the so called "antitaenite" in [45] (this latter term is doubtful, because this is the paramagnetic γ-Fe(Ni, Co) phase in which the Ni content is in the range

Table 3
The unit cell parameters for silicate crystals in the Bjurböle L/LL4 ordinary chondrite obtained by X-ray diffraction.

Silicate crystal	Unit cell parameters			
	a, Å	*b*, Å	*c*, Å	β, °
Olivine	10.2744(5)	6.0125(4)	4.7736(4)	–
Orthopyroxene	18.2819(9)	8.8691(7)	5.1960(7)	–
Ca-rich clinopyroxene	9.763(9)	8.898(9)	5.259(8)	106.2

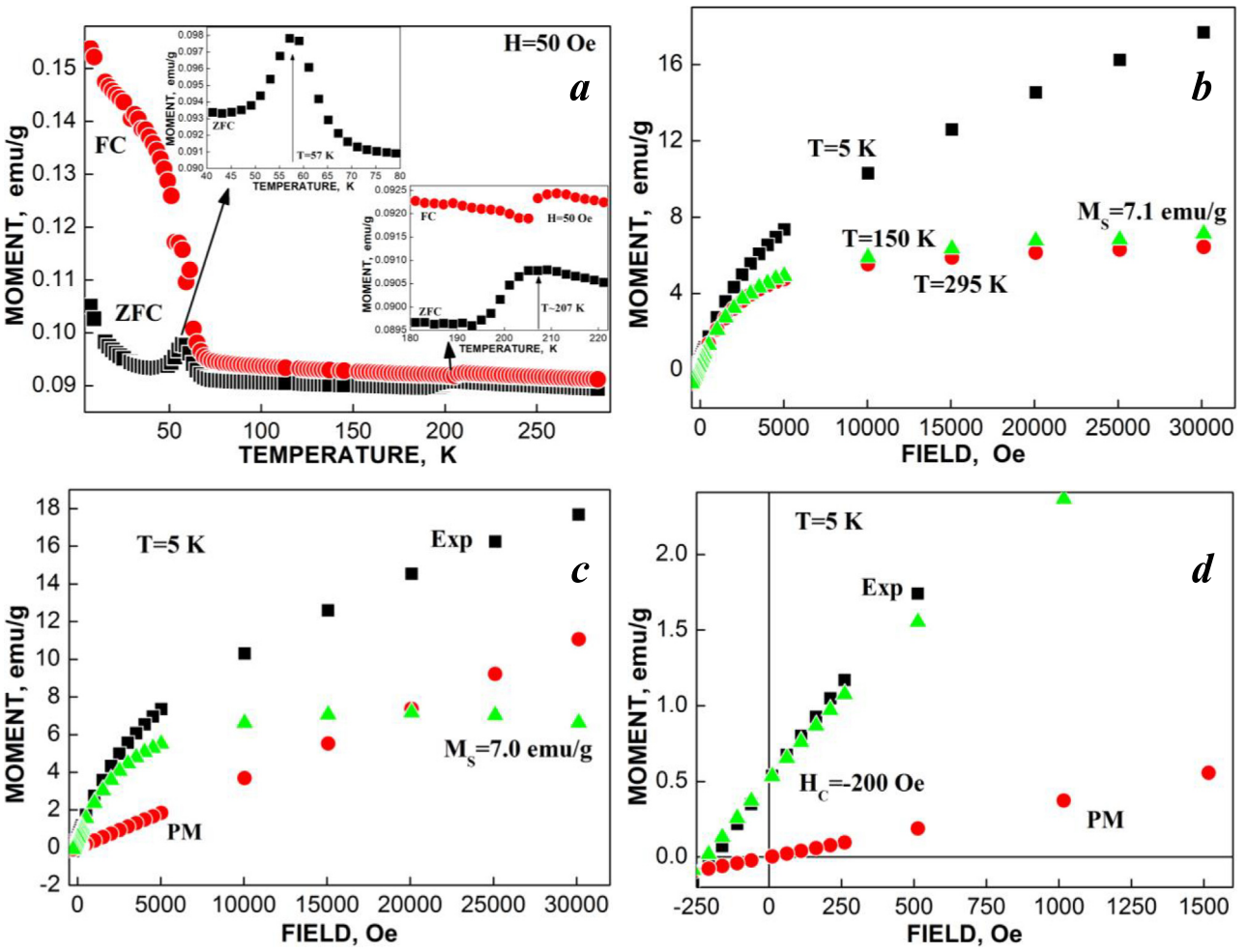

Fig. 6. Zero-field-cooled (**ZFC**) and field-cooled (**FC**) curves (***a***) and isothermal magnetization curves (***b–d***) of the Bjurböle L/LL4 matter. **Exp** is experimental points, **PM** is the paramagnetic contribution, $\mathbf{M_S}$ is the saturation magnetic moment, **H** is the magnetic field, $\mathbf{H_C}$ is the coercive field, **T** is temperature.

~29–~33 at%, which is present in the terrestrial alloys, see, e.g., [46–49], and is in contrast to the authors' claim in [45] that this is a new mineral found in meteorites only). The presence of this component in the Mössbauer spectrum is confirmed also by EDS analysis (see Table 1 and Fig. 3). If we suggest the same Mössbauer effect probabilities (*f*-factors) for all iron-bearing phases, the relative areas of all components are proportional to the relative iron fractions in these phases. Therefore, it is possible to compare the relative areas of spectral components between Bjurböle L/LL4 and some LL and L ordinary chondrites with petrologic types 4 and 6 (Fig. 8). The observed main differences in the relative iron fractions in identical phases in these meteorites correspond to the known differences between ordinary chondrites from the LL and L groups.

Mössbauer hyperfine parameters can reflect small variations in the ^{57}Fe local microenvironments for similar structures. For example, these variations in silicate crystals (olivine, orthopyroxene and clinopyroxene) from different meteorites may be related to different iron and magnesium contents and different Fe^{2+} and Mg^{2+} distributions among the M1 and M2 sites in the same silicates in different ordinary chondrites. For this reason, we compare Mössbauer hyperfine parameters for the M1 and M2 sites in both olivine and orthopyroxene crystals from the Bjurböle L/LL4, Ozerki L6, NWA 6286 LL6 and Kemer L4 ordinary chondrites (Fig. 9). The ΔE_Q values of ^{57}Fe in the M1 and M2 sites in olivine are respectively the same (within the error) for both Bjurböle L/LL4 and Kemer L4 and slightly different (beyond the error) for NWA 6286 LL6 and Ozerki L6. In contrast, the ΔE_Q value of ^{57}Fe in the M1 sites in orthopyroxene in Bjurböle L/LL4 is slightly larger (beyond the error) than that obtained for the other meteorites, while ΔE_Q of ^{57}Fe in the M2 sites are the same for these ordinary chondrites. Therefore, it can be expected that small variations in these ΔE_Q

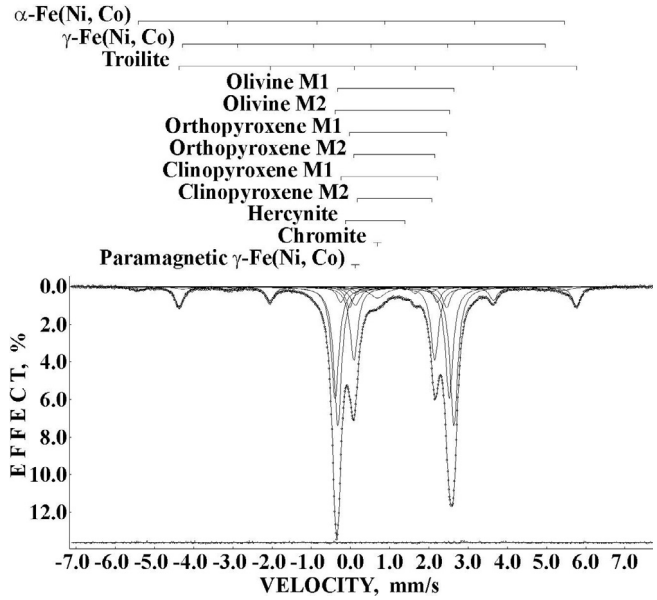

Fig. 7. Mössbauer spectrum of the Bjurböle L/LL4 ordinary chondrite. Indicated components are the result of the best fit. The differential spectrum is shown at the bottom.

values can be related to some differences in both the iron content and the Fe^{2+} distribution among the M1 and M2 sites in the silicate crystals in these meteorites.

A comparison of Mössbauer hyperfine parameters for troilite in the same ordinary chondrites is shown in Fig. 10. The H_{eff} values for troilite in Bjurböle L/LL4, Ozerki L6, Kemer L4 and NWA 6286 LL6 ordinary chondrites are very close. However, the two former meteorites demonstrate slightly larger H_{eff} value especially in comparison with NWA 6286 LL6. It is known that decrease in H_{eff} is related to increase in the Fe vacancies in troilite (see [50]). This probably can be associated with additional spectral components of nonstoichiometric $Fe_{1-x}S$ troilite found in the NWA 6286 LL6 Mössbauer spectrum [34] while this component is absent in the spectrum of Bjurböle L/LL4. It is possible that some additional thermal effects can lead to increase in the Fe vacancies in troilite.

3.6. The Fe^{2+} occupancies in the M1 and M2 sites of silicate crystals

The Fe^{2+} and Mg^{2+} cations distribution among the M1 and M2 sites in silicate crystals is related to their thermal history, shock and reheating in the parent bodies, etc. Therefore, it is important to determine the Fe^{2+} and Mg^{2+} occupancies of the M1 and M2 sites in olivine, orthopyroxene and clinopyroxene (X_{Fe}^{M1}, X_{Fe}^{M2}, X_{Mg}^{M1} and X_{Mg}^{M2}, respectively). Detailed determination of X_{Fe}^{M1} and X_{Fe}^{M2} directly from the XRD data is shown in [51] and references therein. The values of X_{Mg}^{M1} and X_{Mg}^{M2} can be calculated as $1 - X_{Fe}^{M1}$ and $1 - X_{Fe}^{M2}$, respectively. On the other hand, Mössbauer spectroscopy cannot determine these occupancies. However, if we consider equal *f*-factors for all phases, we can estimate the relative Fe^{2+} fractions in the corresponding M1 and M2 sites, using the relative areas associated with the M1 and M2 sites (A^{M1} and A^{M2}, respectively). Therefore, the ratios of Fe^{2+} occupancies of the M1 and M2 sites can be obtained from both XRD and Mössbauer data (X_{Fe}^{M1}/X_{Fe}^{M2} and A^{M1}/A^{M2}, respectively).

The values for Bjurböle L/LL4 are: (a) $X_{Fe}^{M1} = 0.29$, $X_{Fe}^{M2} = 0.24$, $X_{Fe}^{M1}/X_{Fe}^{M2} = 1.21$ (XRD) and $A^{M1}/A^{M2} = 1.24$ (Mössbauer spectroscopy) for olivine, (b) $X_{Fe}^{M1} = 0.09$, $X_{Fe}^{M2} = 0.40$, $X_{Fe}^{M1}/X_{Fe}^{M2} = 0.23$ (XRD) and $A^{M1}/A^{M2} = 0.28$ (Mössbauer spectroscopy) for orthopyroxene and (c) $X_{Fe}^{M1} = 0.28$, $X_{Fe}^{M2} = 0.09$, $X_{Ca}^{M2} = 0.82$, $X_{Fe}^{M1}/X_{Fe}^{M2} = 3.11$ (XRD) and $A^{M1}/A^{M2} = 3.13$ (Mössbauer spectroscopy) for clinopyroxene (X_{Ca}^{M2} is Ca^{2+} occupancy of the M2 sites in Ca-rich clinopyroxene). Thus, ratios of Fe^{2+} occupancies of the M1 and M2 sites determined from XRD and Mössbauer spectroscopy are in a good agreement.

Furthermore, these results can be used for estimation of (i) the distribution coefficient K_D and (ii) the temperature of cation equilibrium distribution T_{eq} for both olivine and orthopyroxene. The K_D is calculated from the XRD data as follows: $K_D = (X_{Fe}^{M1} \times (1 - X_{Fe}^{M2}))/(X_{Fe}^{M2} \times (1 - X_{Fe}^{M1}))$. To calculate K_D from Mössbauer parameters, we have to use the Fa and Fs values as described in [35,51,52]. To determine T_{eq}, we used the equations: (1) $-\Delta G^\circ = R \times T_{eq} \times \ln K_D$ for olivine, where the Gibbs energy $\Delta G^\circ = 20935$ J for olivine, $R = 8.31$ J/K mol (taken from [53]), and (2) $\ln K_D = 0.391–2205/T_{eq}$ for orthopyroxene (taken from [54]). The resulting values of K_D and T_{eq} for olivine and orthopyroxene calculated using XRD and Mössbauer spectroscopy data for Bjurböle L/LL4 in comparison with those obtained for Kemer L4, NWA 6286 LL6 and Ozerki L6 ordinary chondrites are collected in Table 5. It is interesting to note that T_{eq} (obtained using the both techniques) for olivine in Bjurböle L/LL4 is slightly higher than that in Kemer L4 and Ozerki L6, but slightly lower than T_{eq} for olivine in NWA 6286 LL6. On the other hand, T_{eq} (obtained using the both techniques) for orthopyroxene in Bjurböle L/LL4 is higher than that for Kemer L4, comparable with that for NWA 6286 LL6 and lower than T_{eq} for orthopyroxene in Ozerki L6. This may be a result of the Bjurböle specificity as an equilibrated meteorite (ordinary chondrites from petrologic types 4–6), which morphology is close to unequilibrated ordinary chondrites, but in contrast to the latter, with the matter, which was probably undergone to slightly more recrystallization (see [14]). The T_{eq} values for orthopyroxene agree with the earlier

Table 4
Mössbauer parameters of the Bjurböle L/LL4 matter.

Γ, mm/s	δ, mm/s	$\Delta E_Q/2\varepsilon$, mm/s	H_{eff}, kOe	*A*, %	Component[a]
0.403 ± 0.029	0.015 ± 0.014	0.006 ± 0.014	337.4 ± 0.5	2.76	α-Fe(Ni, Co)
0.403 ± 0.029	0.067 ± 0.014	0.550 ± 0.026	287.0 ± 0.9	1.72	γ-Fe(Ni, Co)
0.253 ± 0.029	0.761 ± 0.014	*Not determined*	314.7 ± 0.5	9.35	Troilite
0.234 ± 0.029	1.156 ± 0.014	2.963 ± 0.014	–	30.53	Olivine M1
0.234 ± 0.029	1.063 ± 0.014	2.913 ± 0.014	–	24.53	Olivine M2
0.234 ± 0.029	1.212 ± 0.014	2.473 ± 0.014	–	4.58	Orthopyroxene M1
0.234 ± 0.029	1.118 ± 0.014	2.060 ± 0.014	–	16.09	Orthopyroxene M2
0.234 ± 0.029	0.984 ± 0.014	2.461 ± 0.014	–	3.44	Clinopyroxene M1
0.234 ± 0.029	1.125 ± 0.014	1.909 ± 0.019	–	1.10	Clinopyroxene M2
0.234 ± 0.029	0.625 ± 0.023	1.521 ± 0.047	–	0.61	Hercynite
0.313 ± 0.029	0.124 ± 0.014	–	–	2.70	γ-Fe(Ni, Co) paramag.[b]
0.496 ± 0.029	0.690 ± 0.014	–	–	2.59	Chromite

[a] Components are the same as shown in Fig. 7. [b]Paramagnetic γ-Fe(Ni, Co) phase.

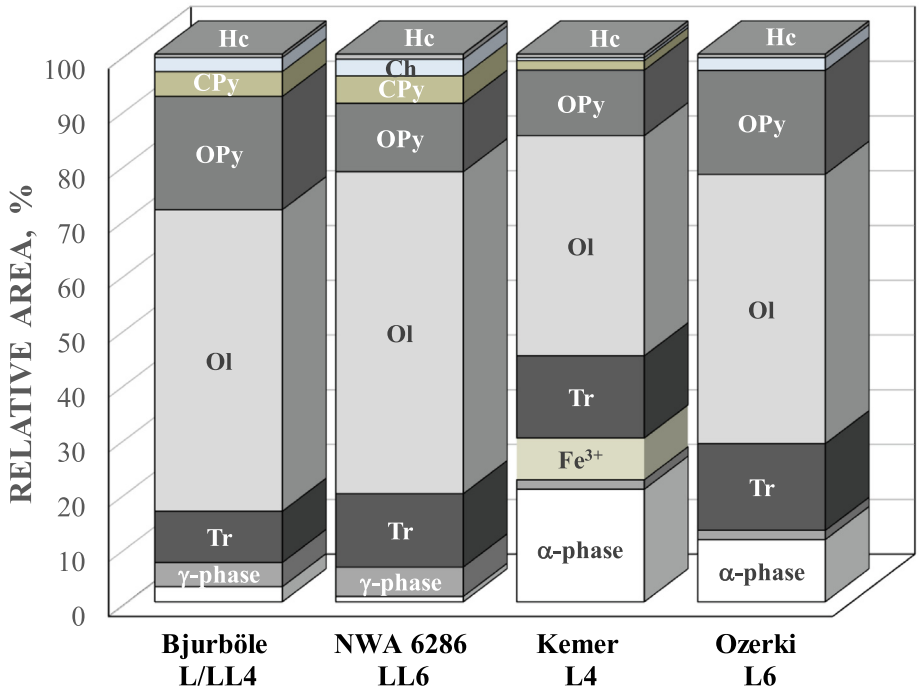

Fig. 8. Comparison of the relative areas of Mössbauer spectral components (the relative iron fractions) for various phases in Bjurböle L/LL4, NWA 6286 LL6, Kemer L4 and Ozerki L6 ordinary chondrites (data for the latter three meteorites were taken from [34,36,37]): **α-phase** is α-Fe(Ni, Co) phase, **γ-phase** is ferromagnetic + paramagnetic γ-Fe (Ni, Co) phases, **Fe^{3+}** is ferric compound, **Tr** is troilite, **Ol** is olivine M1 + M2 sites, **OPy** is orthopyroxene M1 + M2 sites, **CPy** is clinopyroxene M1 + M2 sites, **Ch** is chromite, **Hc** is hercynite.

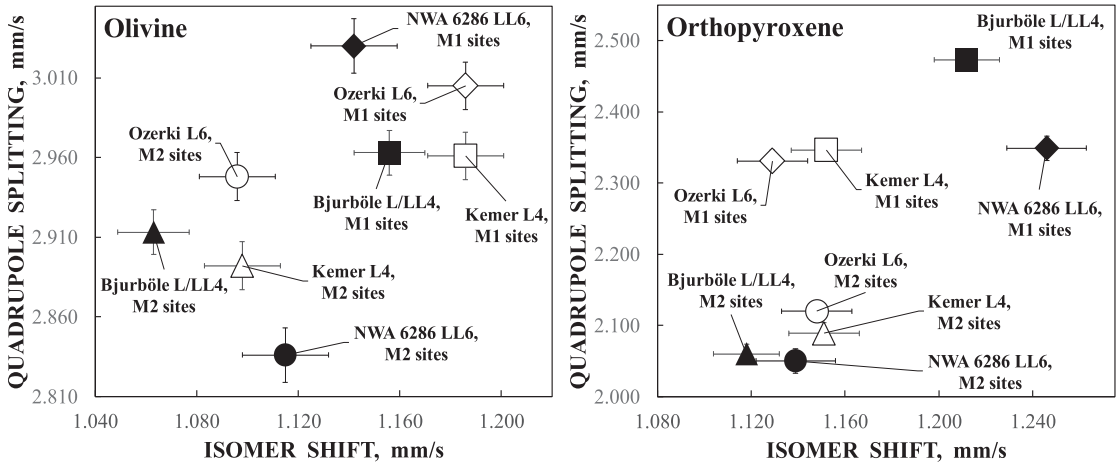

Fig. 9. Comparison of Mössbauer hyperfine parameters for the M1 and M2 sites in olivine and orthopyroxene crystals in Bjurböle L/LL4 (■, ▲), Kemer L4 (□, △), NWA 6286 LL6 (◆, ●) and Ozerki L6 (◇, ○) ordinary chondrites (data for the latter three meteorites were taken from [34,36,37]).

assumption, that this silicate in the Bjurböle meteorite was undergone a higher temperature metamorphism in comparison with some H and L ordinary chondrites [19]. The T_{eq} values for Bjurböle L/LL4 are also in agreement with the average equilibration temperatures for ordinary chondrites with petrologic type 4–6 in the range 859–1050 K and the peak metamorphic temperature range 873–1223 K (see [55]).

3.7. Approaches for the Bjurböle ordinary chondrite classification

There are several approaches to classify ordinary chondrites within H, L and LL groups. Some of them are based on the plots of: (i) the ratio of iron in metallic state (Fe^0) to the total iron in meteorite (Fe^0/Fe) versus fayalite content [56] and (ii) ferrosilite versus fayalite (see, e.g., [57,58]). Using the microprobe analysis data for Bjurböle L/LL4 ordinary chondrite published in [14] (Fa = 26.2 mol%, Fs = 20.7 mol% and Fe^0/Fe = 0.33), we can see the locations of Bjurböle in these two plots as shown in Fig. 11. In the former plot, Bjurböle falls into the L ordinary chondrite region while in the latter plot Bjurböle appeared slightly out of both L and LL regions. If we evaluate Fa and Fs values using the Fe^{2+} occupancies of the M1 and M2 sites in olivine and orthopyroxene in Bjurböle from the XRD data as $(X_{Fe}^{M1} + X_{Fe}^{M2})/2$ for each silicate, we obtain Fa^{XRD} = 26.5 mol% and Fs^{XRD} = 24.5 mol%. The value of Fe^0/Fe = ~0.072 in relative units can be roughly deduced from the relative areas of the Mössbauer spectrum components (see Table 4).

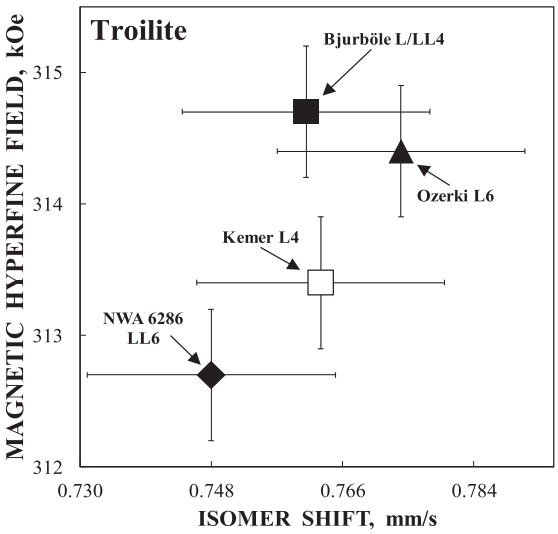

Fig. 10. Comparison of Mössbauer hyperfine parameters for troilite in Bjurböle L/LL4 (■), Kemer L4 (□), NWA 6286 LL6 (◆) and Ozerki L6 (▲) ordinary chondrites (data for the latter three meteorites were taken from [34,36,37]).

Using these values in the plots of Fe^0/Fe vs. Fa and Fs vs. Fa, we can see that Bjurböle falls into the LL regions for ordinary chondrites in both plots (Fig. 11).

Physical techniques such as magnetization measurements and Mössbauer spectroscopy can be also applied for ordinary chondrites classification. Magnetic susceptibility, saturation magnetic moment and some other magnetic parameters may be used for the classification as shown in [17,18]. The mean M_S values for the L, L/LL and LL ordinary chondrites were found as 17.93, 17.51 and 4.11 emu/g, respectively, whereas M_S for Bjurböle was 20.55 emu/g [18] that corresponds to the L and L/LL ordinary chondrites. The M_S = ~7 emu/g determined here for Bjurböle is close to the LL group. Mössbauer spectroscopy was suggested for the classification of ordinary chondrites in [20] and then the relative areas of the Mössbauer spectra components were used for classification in different ways (see, e.g., [52,59–66]). Our approach for ordinary chondrites systematics is based on the plot of (i) the total relative area of spectral components for metal phases plus ferric compound(s) in case of the low weathering grade versus (ii) the total relative area of olivine (M1 and M2 components). The last application of this plot was done for Ozerki L6 classification [36]. This plot was slightly corrected in this work and used for the Bjurböle meteorite classification (see Fig. 12). This meteorite falls into the LL ordinary chondrites region that correlates with our magnetization and XRD data (the latter is shown in Fig. 11, right panel). It should be noticed that this approach is different from those shown in Fig. 11. If we consider the equal *f*-factors for all phases in meteorite, the values in the axes in Fig. 12 in fact equal to the relative Fe fractions in corresponding phases in the studied sample volume of ordinary chondrites. These Fe fractions may not be the same as values of Fa and Fe^0/Fe determined by microprobe analysis.

4. Conclusion

The Bjurböle L/LL4 meteorite, as a "special" representative of the group with a petrologic type 4, was studied by scanning electron microscopy, energy dispersive spectroscopy, Raman spectroscopy, X-ray diffraction, magnetization measurements and Mössbauer spectroscopy. The phase composition of the bulk matter and the unit cell parameters for silicate crystals are determined and compared with the data obtained for the other ordinary chondrites. The Raman spectra indicate the large contents of forsterite and enstatite in silicate matrix. Magnetization measurements show the ferrimagnetic-paramagnetic phase transition in chromite at 57(1) K and a smaller constant (in the temperature range from 5 up to 295 K) saturation magnetic moment M_S = ~7 emu/g which is comparable with those for some LL ordinary chondrites. The ^{57}Fe Mössbauer spectrum of Bjurböle is composed with three magnetic sextets, seven quadrupole doublets and two paramagnetic singlets which are assigned to the corresponding iron-bearing phases. The relative iron fractions in these phases and Mössbauer hyperfine parameters for the M1 and M2 sites in olivine and orthopyroxene as well as for troilite are compared with the similar data obtained for the other L and LL ordinary chondrites and demonstrate some differences. Using the XRD and Mössbauer data, the ratios of Fe^{2+} occupancies of the M1 and M2 sites in silicate crystals are determined. The values obtained by the two independent techniques agree to each other. The temperatures of equilibrium cation distribution for olivine and orthopyroxene are calculated using XRD and Mössbauer results and compared with some other L and LL ordinary chondrites. It is found that T_{eq} for orthopyroxene in Bjurböle L/LL4 is higher than that for Kemer L4 but comparable with T_{eq} for NWA 6286 LL6 and Ozerki L6. Some approaches for the Bjurböle classification using the results of XRD, magnetization measurements and Mössbauer spectroscopy obtained in this work demonstrate that the studied matter is close to the LL ordinary chondrite group.

Table 5
The values of the distribution coefficient and the temperature of equilibrium cation distribution for olivine and orthopyroxene in the selected ordinary chondrites calculated using XRD and Mössbauer spectroscopy.

Ordinary chondrite	XRD		Mössbauer spectroscopy		
	K_D	T_{eq}, K	Fa/Fs, mol%	K_D	T_{eq}, K
Olivine					
Bjurböle L/LL4	1.46	666	26.2	1.34	850
Kemer L4[a]	1.77	441	24	1.77	439
NWA 6286 LL6[b]	1.34	862	29.9	1.28	1006
Ozerki L6[c]	1.58	553	26	1.69	479
Orthopyroxene					
Bjurböle L/LL4	0.148	958	20.7	0.21	1136
Kemer L4[a]	0.10	806	19	0.09	787
NWA 6286 LL6[b]	0.17	1010	23.9	0.18	1052
Ozerki L6[c]	0.24	1213	21	0.24	1202

Data were taken from: [a][37], [b][34] and [c][36].

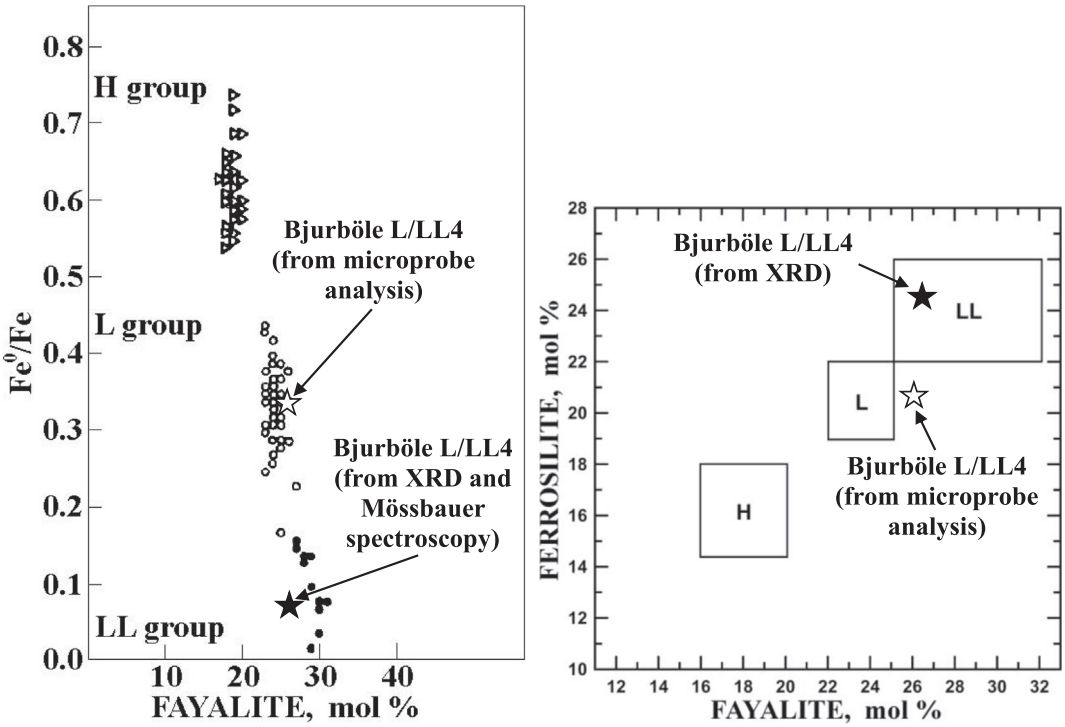

Fig. 11. Classification of ordinary chondrites using the plots of: (left panel) Fe^0/Fe vs. fayalite (adopted from [56]) and (right panel) ferrosilite vs. fayalite (adopted from [59]). Symbol ☆ indicates the positions of the Bjurböle meteorite in these plots based on the data obtained using the microprobe analysis in [14], while symbol ★ indicates the positions of the Bjurböle meteorite evaluated from the XRD and Mössbauer data in this work.

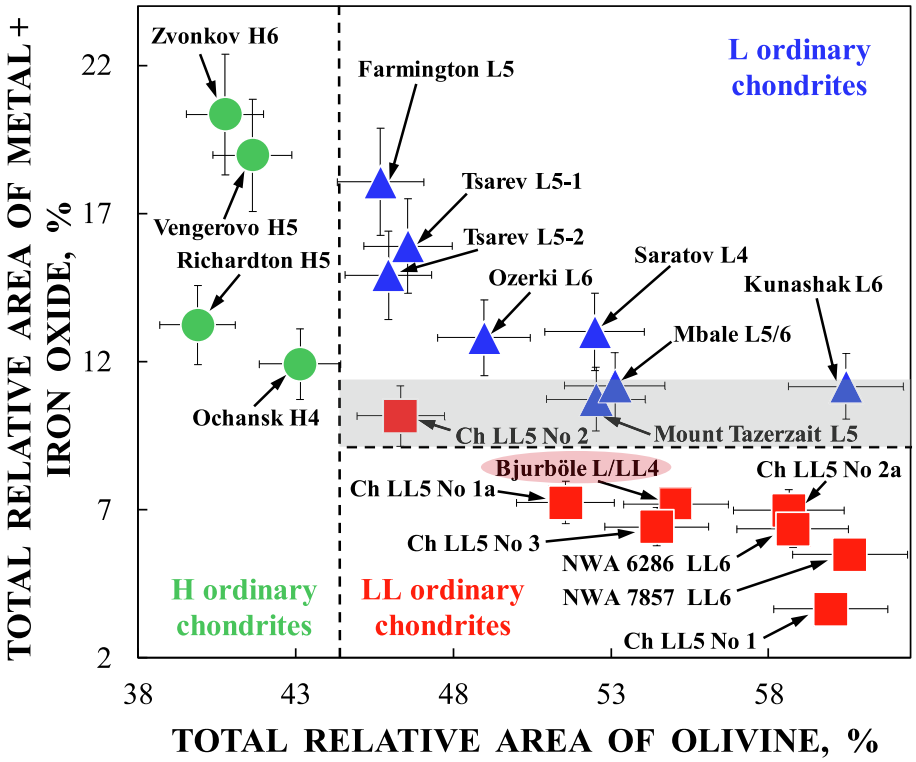

Fig. 12. Approach for ordinary chondrites classification using the relative areas of the Mössbauer spectra components with indication of the Bjurböle meteorite position. **Ch LL5** means the Chelyabinsk LL5 ordinary chondrite with different fragments numbered No 1, No 1a, No 2, No 2a and No 3.

CRediT authorship contribution statement

A.A. Maksimova: Formal analysis, Investigation, Methodology, Writing - review & editing. **E.V. Petrova**: Investigation, Methodology, Writing - review & editing. **A.V. Chukin**: Formal analysis, Investigation, Methodology, Software, Validation, Writing - review & editing. **B.A. Nogueira**: Formal analysis, Investigation, Methodology, Software, Writing - review & editing. **R. Fausto**: Formal analysis, Investigation, Methodology, Writing - review & editing. **Á. Szabó**: Formal analysis, Investigation, Methodology, Software, Writing - review & editing. **Z. Dankházi**: Formal analysis, Investigation, Methodology, Software, Writing - review & editing. **I. Felner**: Formal analysis, Investigation, Methodology, Software, Validation, Writing - review & editing. **M. Gritsevich**: Data curation, Writing - review & editing. **T. Kohout**: Data curation, Writing - review & editing. **E. Kuzmann**: Formal analysis, Data curation, Writing - review & editing. **Z. Homonnay**: Formal analysis, Data curation, Writing - review & editing. **M.I. Oshtrakh**: Supervision, Conceptualization, Project administration, Data curation, Formal analysis, Investigation, Methodology, Software, Validation, Visualization, Writing - original draft, Writing - review & editing.

Declaration of Competing Interest

The authors have no conflict of interest.

Acknowledgements

This work was supported by the Ministry of Science and Higher Education of the Russian Federation, project № FEUZ-2020-0060, and Act 211 of the Government of the Russian Federation, contract № 02.A03.21.0006. The Coimbra Chemistry Centre (CQC; research unit UI0313/QUI/2020) is supported by the Portuguese Science Foundation (FCT) and COMPETE-UE. On behalf of two of us (Á.Sz. and Z.D.) this work was completed in the ELTE Excellence Programme (783-3/2018/FEKUTSRAT) supported by the Hungarian Ministry of Human Capacities. E.K. and Z.H. acknowledge NKFIH-OTKA (the grants № 115784, № 115913 and № 134770). M.G. acknowledges insightful discussions with Jarmo Moilanen and the Academy of Finland project № 325806 "Planetary spectrometry". T.K. acknowledges the Academy of Finland project № 293975. The Zavaritsky Institute of Geology and Geochemistry of the Ural Branch of the Russian Academy of Sciences is supported by the Ministry of Science and Higher Education of the Russian Federation, project № AAAA-A19-119071090011-6 (A.A.M.). This work was carried out within the Agreements of Cooperation between the Ural Federal University (Ekaterinburg) and the University of Coimbra (Coimbra) and between the Ural Federal University (Ekaterinburg) and the Eötvös Loránd University (Budapest).

References

[1] J. Moilanen, J. Kettunen, The revised coordinates for Bjurböle meteorite, Finland, Meteor. Planet. Sci. 51(SI, Suppl. 1) (2016) A470 (Abstract No 6500, 79th Annual Meeting of the Meteoritical Society).
[2] W. Ramsay, L.H. Borgström, Der meteorit von Bjurböle bei Borgå, Bulletin de la Commission Géologique de Finlande 12 (1902) 1–28.
[3] https://www.lpi.usra.edu/meteor/metbull.php?code=5064.
[4] https://www.mindat.org/loc-155472.html.
[5] http://www.somerikko.net/meteoriitit/bjurbole.html.
[6] K.E. Kuebler, H.Y. McSween Jr., Sizes and masses of chondrules and metal–troilite grains in ordinary chondrites: possible implications for Nebular sorting, Icarus 141 (1999) 96–106.
[7] E. Polnau, O. Eugster, M. Burger, U. Krähenbühl, K. Marti, Precompaction exposure of chondrules and implications, Geochim. Cosmochim. Acta 65 (2001) 1849–1866.
[8] J.M. Friedrich, M.-S. Wang, M.E. Lipschutz, Chemical studies of L chondrites. V: Compositional patterns for 49 trace elements in 14 L4–6 and 7 LL4-6 falls, Geochim. Cosmochim. Acta 67 (2003) 2467–2479.
[9] A. Bouvier, J. Blichert-Toft, F. Moynier, J.D. Vervoort, F. Albarède, Pb–Pb dating constraints on the accretion and cooling history of chondrites, Geochim. Cosmochim. Acta 71 (2007) 1583–1604.
[10] H.A. Kovach, R.H. Jones, Feldspar in type 4–6 ordinary chondrites: Metamorphic processing on the H and LL chondrite parent bodies, Meteorit. Planet. Sci. 45 (2010) 246–264.
[11] A.S.G. Roth, K. Metzler, L.P. Baumgartner, I. Leya, Cosmic-ray exposure ages of chondrules, Meteorit. Planet. Sci. 51 (2016) 1256–1267.
[12] B. Mason, Olivine composition in chondrites, Geochim. Cosmochim. Acta 27 (1963) 1011–1023.
[13] G.W. Kallemeyn, A.E. Rubin, D. Wang, J.T. Wasson, Ordinary chondrites: Bulk compositions, classification, lithophile-element fractionations, and composition-petrographic type relationships, Geochim. Cosmochim. Acta 53 (1989) 2747–2767.
[14] R.T. Dodd Jr., M.R. Van Schmus, D.M. Koffman, A survey of the unequilibrated ordinary chondrites, Geochim. Cosmochim. Acta 31 (1967) 921–951.
[15] P. Wasilewski, T. Dickinson, Aspects of the validation of magnetic remanence in meteorites, Meteorit. Planet. Sci. 35 (2000) 537–544.
[16] G. Acton, Q.-Z. Yin, K.L. Verosub, L. Jovane, A. Roth, B. Jacobsen, D.S. Ebel, Micromagnetic coercivity distributions and interactions in chondrules with implications for paleointensities of the early solar system, J. Geophys. Res. 112 (2007) B03S90.
[17] P. Rochette, L. Sagnotti, M. Bourot-Denise, G. Consolmagno, L. Folco, J. Gattacceca, M.L. Osete, L. Pesonen, Magnetic classification of stony meteorites: 1. Ordinary chondrites, Meteorit. Planet. Sci. 38 (2003) 251–268.
[18] J. Gattacceca, C. Suavet, P. Rochette, B.P. Weiss, M. Winklhofer, M. Uehara, J.M. Friedrich, Metal phases in ordinary chondrites: Magnetic hysteresis properties and implications for thermal history, Meteorit. Planet. Sci. 49 (2014) 652–676.
[19] R.W. Dundon, L.S. Walter, Ferrous ion order-disorder in meteoritic pyroxenes and the metamorphic history of chondrites, Earth Planet. Sci. Lett. 2 (1967) 372–376.
[20] W. Herr, B. Skerra, Mössbauer spectroscopy applied to the classification of stone meteorites, in: Meteorite Research. Proceedings of a symposium on meteorite research held in Vienna, Austria, 7–13 August, 1968. Ed. P.L. Millman. D. Reidel Publishing Company, Dordrecht, 1969, pp. 104–122.
[21] P. Duda, P. Rzepecka, M. Jakubowska, M. Woźniak, Ł. Karwowski, J. Gałązka-Friedman, Mössbauer studies of iron sulphides present in ordinary chondrites type LL, Acta Soc. Metheorit. Polon. 8 (2017) 30–39 (in Polish).
[22] A.A. Maksimova, M.I. Oshtrakh, E.V. Petrova, V.I. Grokhovsky, V.A. Semionkin, Study of Chelyabinsk LL5 meteorite fragment with light lithology and its fusion crust using Mössbauer spectroscopy with a high velocity resolution, in: Proceedings of the International Conference "Mössbauer Spectroscopy in Materials Science 2014", Eds. J. Tuček, M. Miglierini, AIP Conference Proceedings, Melville, New York, 2014, 1622, 24–29.
[23] A.A. Maksimova, M.I. Oshtrakh, E.V. Petrova, V.I. Grokhovsky, V.A. Semionkin, The ^{57}Fe hyperfine interactions in the iron bearing phases in different fragments of Chelyabinsk LL5 meteorite: a comparative study using Mössbauer spectroscopy with a high velocity resolution, Hyperfine Interact. 230 (2015) 79–87.
[24] M.I. Oshtrakh, A.A. Maksimova, Z. Klencsár, E.V. Petrova, V.I. Grokhovsky, E. Kuzmann, Z. Homonnay, V.A. Semionkin, Study of Chelyabinsk LL5 meteorite fragments with different lithology using Mössbauer spectroscopy with a high velocity resolution, J. Radioanal. Nucl. Chem. 308 (2016) 1103–1111.
[25] A.A. Maksimova, A.V. Chukin, M.I. Oshtrakh, Revealing of the minor iron-bearing phases in the Mössbauer spectra of Chelyabinsk LL5 ordinary chondrite fragment, in: J. Tuček, M. Miglierini (Eds.), Proceedings of the International Conference "Mössbauer Spectroscopy in Materials Science 2016, 1781, AIP Conference Proceedings. AIP Publishing, Melville, New York, 2016 020016.
[26] A.A. Maksimova, M.I. Oshtrakh, V.I. Grokhovsky, E.V. Petrova, V.A. Semionkin, Mössbauer spectroscopy of H, L and LL ordinary chondrites, Hyperfine Interact. 237 (2016) 134.
[27] M.I. Oshtrakh, A.A. Maksimova, V.I. Grokhovsky, E.V. Petrova, V.A. Semionkin, The ^{57}Fe hyperfine interactions in the iron-bearing phases in some LL ordinary chondrites, Hyperfine Interact. 237 (2016) 138.
[28] R.J. Hill, C.J. Howard, A computer program for Rietveld analysis of fixed wavelength X-ray and neutron diffraction patterns, Australian Atomic Energy Commission Research Report (1986) M112.
[29] M.I. Oshtrakh, V.A. Semionkin, Mössbauer spectroscopy with a high velocity resolution: advances in biomedical, pharmaceutical, cosmochemical and nanotechnological research, Spectrochim. Acta, Part A: Molec. and Biomolec. Spectroscopy 100 (2013) 78–87.
[30] M.I. Oshtrakh, V.A. Semionkin, Mössbauer spectroscopy with a high velocity resolution: principles and applications, in: Proceedings of the International Conference "Mössbauer Spectroscopy in Materials Science 2016" (J. Tuček, M. Miglierini, eds.), AIP Conference Proceedings. AIP Publishing, Melville, New York, 2016, 1781, 020019.
[31] A.A. Maksimova, M.I. Oshtrakh, Z. Klencsár, E.V. Petrova, V.I. Grokhovsky, E. Kuzmann, Z. Homonnay, V.A. Semionkin, A comparative study of troilite in bulk ordinary chondrites Farmington L5, Tsarev L5 and Chelyabinsk LL5 using Mössbauer spectroscopy with a high velocity resolution, J. Mol. Struct. 1073 (2014) 196–201.
[32] A.A. Maksimova, Z. Klencsár, M.I. Oshtrakh, E.V. Petrova, V.I. Grokhovsky, E. Kuzmann, Z. Homonnay, V.A. Semionkin, Mössbauer parameters of ordinary chondrites influenced by the fit accuracy of the troilite component: an example of Chelyabinsk LL5 meteorite, Hyperfine Interact. 237 (2016) 33.

[33] A.A. Maksimova, M.I. Oshtrakh, E.V. Petrova, V.I. Grokhovsky, V.A. Semionkin, Comparison of iron-bearing minerals in ordinary chondrites from H, L and LL groups using Mössbauer spectroscopy with a high velocity resolution, Spectrochim. Acta, Part A: Molec. Biomolec. Spectroscopy 172 (2017) 65–76.
[34] A.A. Maksimova, M.I. Oshtrakh, A.V. Chukin, I. Felner, G.A. Yakovlev, V.A. Semionkin, Characterization of Northwest Africa 6286 and 7857 ordinary chondrites using X-ray diffraction, magnetization measurements and Mössbauer spectroscopy, Spectrochim. Acta, Part A: Molec. Biomolec. Spectroscopy 192 (2018) 275–284.
[35] M.I. Oshtrakh, A.A. Maksimova, A.V. Chukin, E.V. Petrova, P. Jenniskens, E. Kuzmann, V.I. Grokhovsky, Z. Homonnay, V.A. Semionkin, Variability of Chelyabinsk meteoroid stones studied by Mössbauer spectroscopy and X-ray diffraction, Spectrochim. Acta, Part A: Molec. Biomolec. Spectroscopy 219 (2019) 206–224.
[36] A.A. Maksimova, E.V. Petrova, A.V. Chukin, M.S. Karabanalov, I. Felner, M. Gritsevich, M.I. Oshtrakh, Characterization of the matrix and fusion crust of the recent meteorite fall Ozerki L6, Meteorit. Planet. Sci. 55 (2020) 231–244.
[37] A.A. Maksimova, E.V. Petrova, A.V. Chukin, M.S. Karabanalov, B.A. Nogueira, R. Fausto, M. Yesiltas, I. Felner, M.I. Oshtrakh, Characterization of Kemer L4 meteorite using Raman spectroscopy, X-ray diffraction, magnetization measurements and Mössbauer spectroscopy, Spectrochim. Acta, Part A: Molec. Biomolec. Spectroscopy 242 (2020) 118723.
[38] R.J. Reisener, J.I. Goldstein, Ordinary chondrite metallography: Part 2. Formation of zoned and unzoned metal particles in relatively unshocked H, L, and LL chondrites, Meteorit. Planet. Sci. 38 (2003) 1679–1696.
[39] B. Lafuente, R.T. Downs, H. Yang, N. Stone, The power of databases: the RRUFF project, in: T. Armbruster, R.M. Danisi (Eds.), Highlights in Mineralogical Crystallography, Berlin, Germany, W. De Gruyter, 2015, pp. 1–30.
[40] E. Huang, C.H. Chen, T. Huang, E.H. Lin, J. Xu, Raman spectroscopic characteristics of Mg-Fe-Ca pyroxenes, Am. Mineral. 85 (2000) 473–479.
[41] K. Mohanan, S.K. Sharma, F.C. Bishop, A Raman spectral study of forsterite-monticellite solid solutions, Am. Mineral. 78 (1993) 42–48.
[42] A. Chopelas, Single crystal Raman spectra of forsterite, fayalite, and monticellite, Am. Mineral. 76 (1991) 1101–1109.
[43] M. Pencipe, L. Mantovani, M. Tribaudino, D. Bersani, P.P. Lottici, The Raman spectrum of diopside: a comparison between ab initio calculated and experimentally measured frequencies, Eur. J. Mineral. 24 (2012) 457–464.
[44] J. Gattacceca, P. Rochette, F. Lagroix, P.-E. Mathé, B. Zanda, Low temperature magnetic transition of chromite in ordinary chondrites, Geophys. Res. Lett. 38 (2011) L10203.
[45] E. Dos Santos, J. Gattacceca, P. Rochette, R.B. Scorzelli, G. Fillion, Magnetic hysteresis properties and ^{57}Fe Mössbauer spectroscopy of iron and stony-iron meteorites: Implications for mineralogy and thermal history, Phys. Earth Planet. Inter. 242 (2015) 50–64.
[46] Y. Nakamura, M. Shiga, N. Shikazono, Mössbauer study of invar-type iron-nickel alloys, J. Phys. Soc. Jpn. 19 (1964) 1177–1181.
[47] Y. Tino, J. Arai, Mössbauer spectra of the Fe-Ni invar alloys under the influence of non-hydrostatic stress, J. Phys. Soc. Jpn. 36 (1974) 669–674.
[48] Y.V. Baldokhin, V.V. Tcherdyntsev, S.D. Kaloshkin, G.A. Kochetov, Y.A. Pustov, Transformations and fine magnetic structure of mechanically alloyed Fe–Ni alloys, J. Mag. Mag. Mater. 203 (1999) 313–315.
[49] J.F. Valderruten, G.A.P. Alcazar, J.M. Greneche, Study of Fe–Ni alloys produced by mechanical alloying, Phys. B: Condens. Matter. 384 (2006) 316–318.
[50] O. Kruse, Mössbauer and X-ray study of the effects of vacancy concentration in synthetic hexagonal pyrrhotites, Am. Mineral. 75 (1990) 755–763.
[51] A.A. Maksimova, E.V. Petrova, A.V. Chukin, M.I. Oshtrakh, Fe^{2+} partitioning between the M1 and M2 sites in silicate crystals in some stony and stony-iron meteorites studied using X-ray diffraction and Mössbauer spectroscopy, J. Mol. Struct. 1216 (2020) 128391.
[52] M.I. Oshtrakh, E.V. Petrova, V.I. Grokhovsky, V.A. Semionkin, A study of ordinary chondrites by Mössbauer spectroscopy with high-velocity resolution, Meteorit. Planet. Sci. 43 (2008) 941–958.
[53] T.V. Malysheva, Mössbauer Effect in Geochemistry and Cosmochemistry, Moscow, Nauka (1975) 166 (in Russian).
[54] L. Wang, N. Moon, Y. Zhang, W.R. Dunham, E.J. Essene, Fe-Mg order-disorder in orthopyroxenes, Geochim. Cosmochim. Acta 69 (2005) 5777–5788.
[55] R. Kessel, J.R. Beckett, E.M. Stolper, The thermal history of equilibrated ordinary chondrites and the relationship between textural maturity and temperature, Geochim. Cosmochim. Acta 71 (2007) 1855–1881.
[56] W.R. Van Schmus, J.A. Wood, A chemical-petrologic classification for the chondritic meteorites, Geochim. Cosmochim. Acta 31 (1967) 747–765.
[57] K. Keil, K. Fredriksson, The iron, magnesium, and calcium distribution in coexisting olivines and rhombic pyroxenes of chondrites, J. Geophys. Res. 69 (1964) 3487–3515.
[58] A.J. Brearley, R.H. Jones, Chondritic meteorites, In: Planetary Materials, Ed. J.J. Papike. Reviews in Mineralogy, Vol. 36, 1998, chapter 3.
[59] A.A. Maksimova, M.I. Oshtrakh, Ordinary chondrites: what can we learn using Mössbauer spectroscopy?, J. Mol. Struct. 1186 (2019) 104–117.
[60] B.S. Paliwal, R.P. Tripathi, H.C. Verma, S.K. Sharma, Classification of the Didwana-Rajod meteorite: a Mössbauer spectroscopic study, Meteorit. Planet. Sci. 35 (2000) 639–642.
[61] H.C. Verma, K. Jee, R.P. Tripathi, Systematics of Mössbauer absorption areas in ordinary chondrites and applications to newly fallen meteorite in Jodhpur, India, *Meteorit. Planet. Sci.* 38 (2003) 963–967.
[62] H.C. Verma, R.P. Tripathi, Anomalous Mössbauer parameters in the second generation regolith Ghubara meteorite, Meteorit. Planet. Sci. 39 (2004) 1755–1759.
[63] N.N. Elewa, J.M. Cadogan, An ^{57}Fe Mössbauer study of the ordinary chondrite meteorite Lynch 001, Hyperfine Interact. 238 (2017) 4.
[64] J. Galazka-Friedman, M. Wozniak, P. Duda, P. Rzepecka, M. Jakubowska, Ł. Karwowski, Mössbauer spectroscopy – a useful method for classification of meteorites?, Hyperfine Interact. 238 (2017) 67.
[65] M. Woźniak, J. Gałązka-Friedman, P. Duda, M. Jakubowska, P. Rzepecka, Ł. Karwowski, Application of Mössbauer spectroscopy, multidimensional discriminant analysis, and Mahalanobis distance for classification of equilibrated ordinary chondrites, Meteorit. Planet. Sci. 54 (2019) 1828–1839.
[66] J. Gałązka-Friedman, M. Woźniak, P. Bogusz, M. Jakubowska, Ł. Karwowski, P. Duda, Application of Mössbauer spectroscopy for classification of ordinary chondrites – different database and different methods, Hyperfine Interact. 241 (2020) 20.